Age-Related Changes in D_2 Receptor Binding with Iodine-123-Iodobenzofuran SPECT

Masanori Ichise, James R. Ballinger, Fumiko Tanaka, Morris Moscovitch, Peter H. St. George-Hyslop, Dennis Raphael and Morris Freedman

Department of Nuclear Medicine, Mount Sinai Hospital; Department of Nuclear Medicine, Princess Margaret Hospital; Behavioral Neurology Program and Rotman Research Institute of Baycrest Center for Geriatric Care; and University of Toronto, Toronto, Ontario, Canada

The purpose of this study was to evaluate the effects of age on D_2 receptor binding with ^{123}I-iodobenzofuran (IBF) SPECT. **Methods:** Subjects were 40 healthy volunteers (age 19–83 yr), including 6 who had test/retest studies. Scans were acquired with a triple-head SPECT camera 3 hr postinjection of IBF (300 MBq). Striatal regions (caudate and putamen) were defined by two different region-of-interest (ROI) sets consisting of large volumes [(CLVs), 2.2 and 6.6 ml] and small volumes [(SVs), 0.6 and 1.3 ml]. D_2 binding ($Rv = V_3/V_2$) was quantified using our previously proposed multilinear regression technique. Effects of age on D_2 binding were evaluated by fitting linear, exponential and logarithmic models. **Results:** The mean Rvs were 26% lower than LV for both putamen and caudate than the corresponding values from the SV due to the partial-volume effect. Although the identifiability of Rv using SV deteriorated slightly, the test/retest reproducibility of Rv measurements was equally excellent for LV and SV. The mean Rvs were 11% higher for putamen compared with those for caudate. D_2 binding declined significantly with age ($p < 10^{-5}$) for all three models. The nonlinear models were slightly superior to the linear model in describing the relationship between Rv and age. In these models, D_2 binding declined with age, equally for caudate and putamen at 7%–13% per decade; the decline was progressively smaller with age. **Conclusion:** IBF SPECT permitted reliable measurements of D_2 binding in the caudate or putamen separately using small ROI volumes that significantly improved the quantitation loss from the partial-volume effect. Our results agreed with previous PET and postmortem findings of D_2 binding losses with age. However, these age effects may be nonlinear. Age-related changes in D_2 binding must be taken into consideration in clinical IBF SPECT investigations.

Key Words: iodine-123-iodobenzofuran; dopamine D_2 receptors; aging; dopamine SPECT.

J Nucl Med 1998; 39:1511–1518

SPECT imaging of dopamine D_2 receptors is a promising technique with several potential clinical applications (*1*). The widespread availability and both lower capital and operating costs of SPECT compared with PET suggest that this technique may become an important clinical tool. In particular, D_2 SPECT investigations using ^{123}I-labeled benzamide analogs such as ^{123}I-iodobenzamide (IBZM) and ^{123}I-iodobenzofuran (IBF) have been successfully conducted in patients with movement disorders such as Parkinson's disease, multiple system atrophy and Huntington's disease (*2–4*). In addition, D_2 SPECT imaging may be used to predict response to L-DOPA therapy because L-DOPA requires the presence of intact dopamine receptors to exert a therapeutic effect (*5*).

IBF binds reversibly to D_2 receptors with higher affinity compared with IBZM, provides higher image contrast and is suited for quantitative receptor studies (*6,7*). Previously, we showed that the feasibility of noninvasive measurements of a D_2 binding parameter $Rv = V_3/V_2$ and quantitative IBF SPECT without blood data were reliable and reproducible (*7*). Thus, IBF SPECT may be used to evaluate the significance of serial changes in D_2 binding in patients with progressive extrapyramidal diseases. However, meaningful interpretation of the results of such an investigation must take into consideration potentially confounding changes in D_2 binding caused by normal aging. In fact, postmortem evidence suggests that nigrostriatal dopaminergic pathways may be the system most vulnerable to the effects of aging (*8–13*). Most in vivo investigations of aging effects on D_2 receptors to date have been conducted with PET and have consistently shown age-related decreases in striatal D_2 binding (*14–19*). A few previous D_2 SPECT studies, including ours (*2,4,6*), have also incorporated evaluation of age effects. Although these studies have generally shown reductions in D_2 binding with age, the results were limited by either the small number or the narrow age range of the subjects studied.

The purpose of this study was therefore to evaluate the effects of age on D_2 binding with IBF SPECT in a substantial number of subjects with a wide age range, including the elderly. In this study, we sought to evaluate regional effects of age on Rv in the head of caudate and the body of putamen separately because these striatal subregions receive topographically different nigrostriatal projections with differing pathophysiological implications (*20*). However, errors in quantitative measurements involving small structures such as the caudate and the putamen may be accentuated by such factors as partial-volume effects, statistical noise in the emission counts and inaccuracies in region of interest (ROI) placement. Therefore, we examined the effects of two different ROI sizes on Rv in terms of relative quantitation losses due to partial-volume effects and identifiability, as well as the test/retest reproducibility of Rv measurements.

MATERIALS AND METHODS

Subjects

Forty age-matched (19 women, mean age 45 ± 20 yr; 21 men, mean age 51 ± 20 yr) healthy volunteers (age range 19–83 yr) participated in this study. None of the subjects had current or past history of neuropsychiatric disorders or family history of movement disorders on the basis of a screening interview, and they were free of drugs for at least 3 mo before the study. Twenty were recruited in our previous studies, including 6 who had test/retest studies (*6,7*), and the remaining 20 were recruited for this study. All subjects older than 50 yr had normal MRI of the head, electroencephalogram and Mini Mental Status Examination (*21*). Additionally, these older subjects were evaluated for extrapyramidal motor function using Part III of the Unified Rating Scale for

Received Aug. 20, 1997; revision accepted Dec. 2, 1997.

For correspondence or reprints contact: Masanori Ichise, MD, Room 635, Nuclear Medicine, Department of Medical Imaging, Mount Sinai Hospital, 600 University Ave., Toronto, Ontario, Canada M5G 1X5.

Parkinson's Disease (UPDRS) (*22*). None of them had significant extrapyramidal deficits as determined by the criteria used previously (UPDRS scores: resting tremor of 1+ or greater and/or 2+ or greater rigidity) (*23*). All subjects gave written informed consent. The project was approved by the Human Subjects Review Committee of the University of Toronto.

Labeling of ^{123}I-Iodobenzofuran

Labeling of ^{123}I-IBF was performed as described previously (*6*). The radiochemical yield was 86.3% ± 6.3%, and the radiochemical purity was 97.2% ± 2.4%. Retrospective sterility testing was negative.

SPECT Imaging

Imaging was performed using a triple-head SPECT system (Prism 3000XP; Picker International, Inc., Cleveland, OH) equipped with ultra-high-resolution fanbeam collimators and interfaced to a dedicated computer (Odyssey VP; Picker International). Each subject received a bolus injection of 300 ± 41 MBq (8.1 ± 1.1 mCi) IBF intravenously. For 20 subjects, scans were acquired every 5 min for 180 min. Six of these subjects had a second IBF SPECT study 1 wk later, as described previously (*7*). For the remaining 20 subjects, scans were acquired every 5 min 0–20, 50–70 and 160–180 min postinjection. For each scan, 120 7.5-sec projection images were obtained using 3° intervals on a 128 × 128 matrix over 360° by rotating each head 120°. The radius of rotation was fixed at 13.5 cm. Four fiducial markers containing 2 μCi ^{99m}Tc were taped, two on each side of the subject's head at the level of the canthomeatal line (CML), throughout the entire period of experiment. FWHM of the system was 9.1 mm in water at the center of the field of view. The mean sensitivity of the system was 612 ± 12 cpm/μCi and varied less than 2% and 5% within and between experiments, respectively. Dead-time count losses over this activity range were negligible. Before and after the IBF study, subjects were given 400 mg potassium perchlorate orally.

SPECT images were reconstructed every 10 min on a 64 × 64 matrix. One-pixel-thick (4.33-mm) transaxial slices from the vertex of the brain to the level of the CML, as identified by the fiducial markers, were reconstructed parallel to the CML using a three-dimensional Butterworth postreconstruction filter (order 10, cutoff frequency 0.25) after applying a ramp backprojection filter. Attenuation correction was performed by assuming uniform attenuation equal to that of water (μ = 0.15 cm^{-1}) within an ellipse drawn around the skull, as identified by the fiducial markers.

Image Data Analysis

To evaluate the effects of ROI size on Rv measurements, two different ROI sets were used. *Large volume (LV) set:* From each set of transaxial images, four consecutive slices (1.73 cm thick) corresponding to the highest signal in the basal ganglia were summed. ROIs were placed on this summed image by using templates over the basal ganglia (area = 5.54 cm^2, volume = 9.60 cm^3), the head of caudate (area = 1.27 cm^2, volume = 2.20 cm^3) and the body of putamen (area = 3.82 cm^2, volume = 6.6 cm^3) in each hemisphere and the frontal cortex (area = 10.23 cm^2, volume = 17.70 cm^3) (Fig. 1). The irregular shapes of these templates were created by outlining the transaxial section of the basal ganglia, caudate, putamen and frontal cortex, respectively, on slice number 8 in the *Coplanar Stereotaxic Atlas of the Human Brain* (*24*). *Small volume (SV) set:* From each set of transaxial images, two consecutive slices (0.865 cm thick), as opposed to four for LV, corresponding to the middle of the basal ganglia were summed. ROIs were then placed using the same templates used in LV over the basal ganglia (volume = 4.80 cm^3) in each hemisphere and the frontal cortex (volume = 8.85 cm^3). Note that volumes of these regions were reduced by half compared with LV. Additionally, a small circular ROI over the head of caudate (area = 1.27 cm^2, volume = 0.60 cm^3) and a small elliptical ROI over the body of putamen (area = 3.82 cm^2, volume = 1.3 cm^3) were placed in each hemisphere (Fig. 1).

FIGURE 1. Transaxial IBF SPECT image with typical ROI sets. FC = frontal cortex. LV (right): RBG = right basal ganglia, RCD = right caudate and RPT = right putamen; and SV: LBG = left basal ganglia, Lcd = left caudate and Lpt = left putamen.

ROI placement depended on visual identification of anatomic regions aided by the stereotaxic atlas and MRI scan, when applicable. For both LV and SV, the ROI over the basal ganglia was placed first and then striatal subregions were fitted within. Frontal cortex ROI placement was also guided by the first 10-min IBF scan, which reflects mostly regional cerebral flow (rCBF). All ROIs were applied by the same individual to eliminate interoperator variation. The mean coefficient of intraoperator variability in the outcome measure Rv was 3.3% ± 0.6%. Average counts per pixel from each region were decay corrected to the time of injection.

Quantification of D_2 Binding

D_2 binding was quantified using our previously proposed multilinear regression technique (*6,7*), which permits measurement of $R_v = V_3/V_2$, for radioligands that reversibly bind to receptors without blood data according to the equation,

$$\frac{\int_0^t C_{BG}(t)dt}{C_{BG}(t)} = \left(\frac{a}{a'}\right)\frac{\int_0^t C_{FC}(t)}{C_{BG}(t)} + \left(-\frac{ab'}{a'}\right)\frac{C_{FC}(t)}{C_{BG}(t)} + b, \quad \text{Eq. 1}$$

in which $C_{BG}(t)$ and $C_{FC}(t)$ represent time-activity measurements in the basal ganglia and frontal cortex, respectively, and a, a', b and b' are constants. Rv is related to the partial regression coefficient a/a' in Equation 1, the binding potential (Bp = B_{max}/K_d) and the kinetic parameters k_3 and k_4 as follows (*7*):

$$R_V = \frac{V_3}{V_2} = \frac{a}{a'} - 1 = \frac{Bp}{V_2} = \frac{k_3}{k_4}. \quad \text{Eq. 2}$$

The b in Equation 1 reaches constant after some time t* when the transport of ligand from plasma to tissue becomes unidirectional. This time point was estimated by examining the residual values for outliers after performing multilinear regression analysis as described previously (*7*). For all subjects, Rv was determined from the datasets obtained 0–20, 50–70 and 160–180 min postinjection. Final Rv values were obtained by averaging the right and

TABLE 1
Mean Distribution Volume Ratios of 40 Healthy Subjects

	Basal ganglia		Caudate		Putamen	
	LV	SV	LV	SV	LV	SV
Mean	2.49*	2.70	2.26*	2.93	2.57*	3.24
s.d.	0.72	0.70	0.68	0.75	0.76	0.80

*Significantly lower ($p < 10^{-5}$) compared with the corresponding values for SV.
LV = large volume region-of-interest set; SV = small volume region-of-interest set.

left Rv values as opposed to measuring Rv values from the time-activity data averaged between the two sides, as was done previously (*7*).

Identifiability of Rv through multilinear regression analysis was assessed by examining the standard errors of the estimate of the partial regression coefficient a/a′ expressed in percentage of estimate (%SE). These standard errors are a measure of the identifiability of the parameter by multilinear regression analysis (*7*). Smaller values of these standard errors denote higher parameter identifiability.

Statistical Analysis

Because the Rv and %SE values were all normally distributed, parametric statistical tests were used. Analysis of variance was used to compare Rv and %SE between groups. Both region and ROI set were treated as a within-subject (repeated measures) factor. Individual means were compared by a posthoc Sheff test, which corrects for multiple comparisons (*25*). Two-tailed Student's t-tests (paired samples) were used to compare the mean Rv values between test and retest, as well as the test/retest reproducibility of Rv measurements between LV and SV. The test/retest reproducibility of Rv measurements was assessed by calculating the intraclass correlation coefficient (ρ), as described previously (*7*). This coefficient is an estimate of the reliability of the two sets of measurements, and hence it is an indication of the test/retest reproducibility of Rv measurements. It varies from 0 (no reproducibility) to 1 (total reproducibility). Statistical significance was defined as $p < 0.05$. Summaries of study variables were expressed as mean ± s.d. All statistical analyses were implemented in STATISTICA (StatSoft, Inc., Tulsa, OK).

Age-Effect Analysis

Age-effect analysis was done in two steps. A limited set of analyses were done first for men and women separately. This first-step analysis was limited in that only a linear model was fitted for Rv determined from the SV. In the second step, a complete set of analyses were done for men and women combined into a single group to increase statistical power. This complete set of analyses included all linear and nonlinear models, described below, using Rv determined from both LV and SV. All age-effect analyses were done for a set of regions consisting of caudate and putamen. A preliminary evaluation of the present data suggested that the age-related decline of D_2 binding might not be simply linear, but it might show a slower decline in the older individuals than in younger ones. The relationships between Rv (y) and age (x) were therefore evaluated by performing both linear and nonlinear regression analyses. The biological mechanisms underlying the apparent nonlinear effects of age on D_2 binding is unclear. Therefore, the purpose of nonlinear modeling was simply to fit a few nonlinear functions that might show a slower decline of D_2 binding with age. We included the following three models:

$$y = -Ax + B, \quad \text{Eq. 3}$$

$$y = A\exp(-\lambda_1 x) + B\exp(-\lambda_2 x), \quad \text{Eq. 4}$$

$$\frac{dy}{dx} = -A\left(\frac{1}{x}\right) \text{ or } y = -A\ln x + B. \quad \text{Eq. 5}$$

Equation 3 is a simple linear model with a constant age-related decline rate. In Equation 4, on the other hand, the decline is characterized by a sum of two exponentials with faster (λ_1) and slower (λ_2) time constants ($\lambda_1 > \lambda_2$). Finally, Equation 5 assumes that the rate of decline is proportional to an inverse of age so that the decline rate is, like Equation 4, smaller with age. To evaluate the quality of fit or suitability of these equations, plots of residuals, correlation coefficients (r), coefficients of determination (γ) and Akaike information criterion (AIC) (*26*) were used. Coefficients of determination and AIC were calculated as follows:

$$\gamma = \frac{SST - SSR}{SST} \quad \text{Eq. 6}$$

$$AIC = N\ln(SSR) + 2P \quad \text{Eq. 7}$$

in which *SST*, *SSR*, N and P are the total sum of squares, the residual sum of squares, the number of data points and the number of parameters, respectively. Coefficients of determination are a measure of the fraction of total variance accounted for by the model, and a γ value close to 1.0 indicates that the model accounts for almost all of the variability in Rv. AIC, on the other hand, is based on maximum likelihood estimation, and lower AIC values denote a more suitable model in fitting the experimental data. All nonlinear regression analyses were implemented in SCIENTIST (MicroMath Scientific Software, Salt Lake City, UT).

RESULTS

Rv and ROI Size

All SPECT studies were technically adequate. Examination of the residuals after multilinear regression analysis according to Equation 1, including all data points, showed no outliers, and, hence, all data points were included in the analysis. Multilinear regression analysis was highly significant with the level of significance at least $p < 10^{-4}$ across all subjects. Table 1 summarizes the mean Rv values from the two ROI sets. The mean Rv values using LV for caudate and putamen were lower by 27% and 26%, respectively, compared with the corresponding Rv values using SV ($p < 10^{-5}$). These differences suggest a significant quantitation loss for LV compared with SV from partial-volume effects. There were no differences of the mean Rv values, all inclusive of region (basal ganglia, caudate and putamen) and ROI set (LV and SV), between men (2.75 ± 0.84) and women (2.64 ± 0.91) (analysis of variance, $p = 0.3$). The mean Rv values (LV/SV) were higher (14%/11%) for putamen (2.57 ± 0.76/3.24 ± 0.80) compared with caudate (2.26 ± 0.68/2.93 ± 0.75; $p < 0.01$).

Rv was well identified with %SE values ranging from 3.1% to 4.3%. There were no differences of the mean %SE values for basal ganglia between LV (3.2% ± 1.7%) and SV (3.1% ± 1.7%) ($p > 0.999$). However, the mean %SE values (LV/SV)

TABLE 2
Reproducibility of Test/Retest Volume Ratio Measurements

Study no.	Basal ganglia		Caudate		Putamen	
	Test	Retest	Test	Retest	Test	Retest
	Large volume region-of-interest set					
2	3.43	3.01	3.11	2.66	3.56	3.15
8	2.98	2.70	2.82	2.35	3.06	2.90
10	1.94	2.13	1.73	1.99	2.02	2.18
22	3.43	4.20	2.95	3.65	3.67	4.33
23	2.48	2.47	2.25	2.34	2.52	2.57
27	3.67	3.58	3.32	3.27	3.87	3.76
Mean ± s.d.	2.99 ± 0.67	3.01 ± 0.76*	2.69 ± 0.60	2.71 ± 0.63*	3.12 ± 0.73	3.15 ± 0.79*
Reproducibility (ρ)	0.85		0.78		0.90	
	Small volume region-of-interest set					
2	3.70	3.51	3.78	3.76	4.32	4.12
8	3.20	3.20	3.62	3.19	3.65	3.92
10	2.17	2.25	2.26	2.54	2.63	3.30
22	3.73	4.45	3.83	4.60	4.46	5.50
23	2.72	2.65	2.85	2.90	3.22	3.01
27	3.30	3.62	3.63	3.64	3.72	4.40
Mean ± s.d.	3.13 ± 0.60	3.28 ± 0.77*	3.33 ± 0.63	3.44 ± 0.73*	3.66 ± 0.68	4.04 ± 0.88*
Reproducibility (ρ)	0.89		0.85		0.72	

*No significant difference between test and retest.
ρ = intraclass correlation coefficient.

for both caudate and putamen were higher for SV compared with the corresponding values for LV: caudate (3.5% ± 1.6%/4.2% ± 1.8%) and putamen (3.4% ± 1.8%/4.3% ± 2.4%; $p < 0.05$). With SV, therefore, the identifiability of Rv for both caudate and putamen deteriorated. However, the magnitude of this deterioration was small (an increase in the mean %SE value by 1).

Table 2 summarizes the individual and mean Rv values and the values of intraclass correlation coefficients (ρ) from the two ROI sets for the subgroup of six subjects who had test/retest studies. There were no differences in the mean Rv values for both LV and SV between test/retest ($p > 0.1$). Furthermore, there were no differences in the mean ρ values between LV (0.84 ± 0.06) and SV (0.82 ± 0.09) ($p = 0.8$). The test/retest reproducibility of Rv measurements was equally excellent for LV and SV.

Age Effect

Using the linear model, Rv (r values: caudate/putamen) as determined from the SV declined significantly with age for both men (−0.76/−0.77) and women (−0.83/−0.86). All linear correlations had the level of significance of at least $p < 10^{-4}$. The rates of Rv decline per decade (men/women) were similar between men and women as well as between the caudate (7.6%/7.6%) and the putamen (7.2%/8.2%). Because both the age effects on Rv and the mean Rv values (caudate/putamen) were similar between men (3.00 ± 0.81/3.26 ± 0.83) and women (2.85 ± 0.67/3.22 ± 0.78) ($p > 0.5$), we combined men and women into a single group to increase statistical power in the subsequent more-detailed analyses.

In the single group in which men and women were combined, Rv (r values: LV/SV) declined significantly with age by the linear model for both caudate (−0.80/−0.76) and putamen (−0.78/−0.80). All linear correlations had the level of significance of at least $p < 10^{-5}$. Figure 2 illustrates typical IBF images of young and old healthy subjects. Figure 3 (A and D) illustrates the selected relationships between Rv as determined from the SV and age by the linear model for caudate and putamen, respectively. The rates of Rv decline per decade (LV/SV) were similar between the caudate (9.0%/7.6%) and the putamen (8.7%/7.7%). The decline rates in the caudate or the putamen were 1.5% higher for LV than SV. The two nonlinear regression analyses were also highly significant ($p < 10^{-5}$). Thus, by the biexponential model, Rv (r values: LV/SV) declined significantly with age for both caudate (−0.81/−0.78) and putamen (−0.79/−0.81). By the logarithmic model, Rv (r values: LV/SV) declined significantly with age for both caudate (−0.80/−0.78) and putamen (−0.78/−0.81). Figure 3 (B, C, E and F) illustrates the selected relationships between Rv as determined from the SV and age by the two nonlinear models for caudate and putamen, respectively. The biexponential model reduced to a monoexponetial plus a constant because the slower component had a time constant close to zero ($\lambda_2 < 10^{-8}$). This component was negligible in magnitude compared with the values of $\lambda_1 \cong 2 \times 10^{-2}$. Plots of residuals show an apparently random distribution for all three models. Table 3 summarizes r, γ and AIC values for the three models. The γ values indicate that age accounted for approximately 63% of the total variability in Rv for all three models. Thus, there was considerable intersubject variability in Rv, apart from the age effect. Although the overall quality of fit was similar between the three models, the mean absolute r values and mean γ values were both slightly higher for exponential and logarithmic models compared with the linear model (Table 3). Mean AIC values were lower for the logarithmic model compared with the linear model (Table 3). Thus, as evident from Figure 3 and Table 3, nonlinear modeling of the age effect on D_2 binding was slightly superior to linear modeling. However, the differences between the logarithmic and exponential fits were subtle. Using the logarithmic model, the percent Rv decline (LV/SV) during 21–30 yr and 61–70 yr for caudate were 13.5%/11.7% and 8.7%/6.9% and putamen were 13.2%/11.8% and 8.4%/7.0%, respectively. Therefore, the rates of decline were similar be-

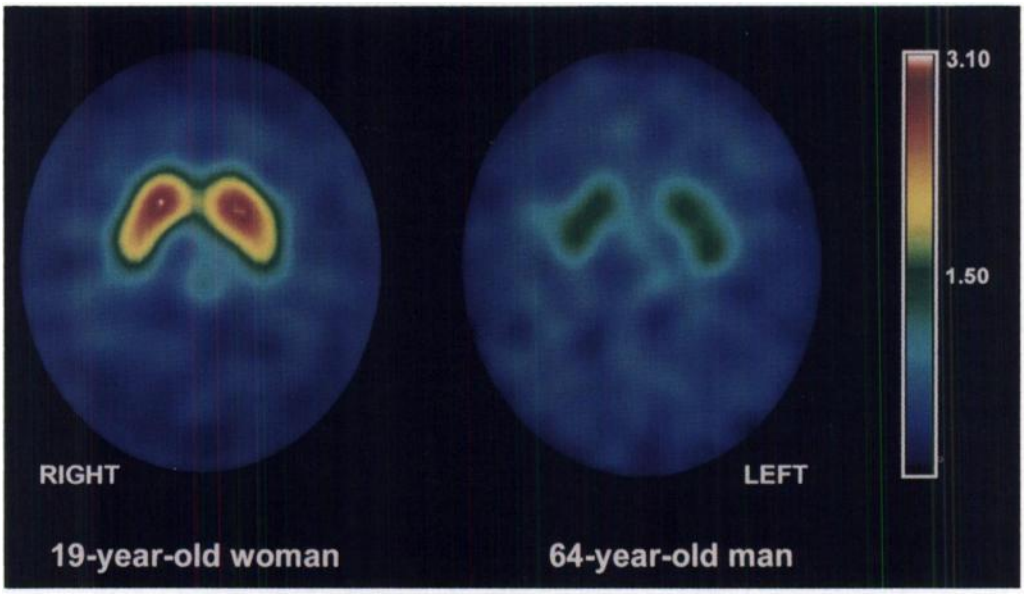

FIGURE 2. Transaxial IBF SPECT images obtained 160–170 min postinjection at the level of the striatum of 19-yr-old woman and 64-yr-old man. Relative iodobenzofuran uptake in the striatum is markedly higher for younger subject (left) than for older subject (right). Image intensity has been adjusted so that striatal activity roughly reflects relative differences in mean basal ganglia Rv values between the two subjects (left image Rv = 3.06, right image Rv = 1.49), although these images are not a parametric map.

tween the caudate and the putamen, as in the linear model, but they were progressively smaller with age as opposed to the rates being constant in the linear model. As in the case of the linear model, the percentage decline rates in the caudate or the putamen were approximately 1.5% higher for LV than SV.

DISCUSSION

Rv and ROI Size

Rv is relatively unaffected by such factors as rCBF and peripheral ligand clearance (*6*). In addition, Rv is practically independent of intersubject variability in terms of body weight, injected IBF dose or percentage brain IBF uptake because Rv is calculated from relative time-activity data of brain tissues. Other advantages and limitations of the use of Rv, particularly as an outcome measure of receptor density, have been discussed previously (*7*).

The reproducibility of Rv measurements in the caudate or the putamen using SV was excellent, although the identifiability of Rv slightly deteriorated. In the ^{18}F-fluorodopa PET study reported by Vingerhoets et al. (*27*), however, reproducibility of Ki measurements (^{18}F-fluorodopa uptake rate constants) from the smaller caudate or putamen ROIs was lower (80%) compared with that from the larger striatal ROI (90%). Reproducibility of these measurements would be lowered by increased statistical noise in emission counts, errors in ROI repositioning and/or head motion during the scan. The lack of significant deterioration in the reproducibility of Rv measurements with SV in this study may have been due to generally favorable emission counts with IBF. IBF provides high target-to-background contrast, and the long physical half-life of ^{123}I (13 hr) permits imaging 3 hr postinjection with only a minor loss of activity as a result of decay. Additionally, our technique of SV placement, whereby placement of small ROIs was guided by the basal ganglia, probably minimized repositioning errors, and the relative contribution of these errors to the intra- and intersubject variances may have been insignificant. With IBF SPECT, therefore, SV ROIs may be a method of choice because quantitation loss from the partial-volume effect is significantly improved and the reliability of Rv measurements is not affected to a substantial degree. However, SV ROIs may be more prone to degradation of data by head motion.

In this study, MR images, which were available only for the 16 older subjects, were used, in addition to the stereotaxic atlas, to visually aid ROI placement without resorting to MRI–SPECT image coregistration. Image coregistration generally should improve the accuracy of ROI placement on the functional image. However, in the recently reported PET study by Wang et al. (*28*), ROIs selected directly from PET images, on which there is a high target-to-background contrast as in D_2 images, were essentially identical to those obtained from coregistered MR images. Therefore, the potential bias introduced in this study caused by the use of MRI only for the older subjects was probably insignificant. The roughly 1.5% higher age-related decline in Rv from the LV than the SV found in this study might have been due to age-related striatal atrophy in our subjects. Previous ^{18}F-fluorodopa PET studies (*27*) have also shown greater age effects on striatal ^{18}F-fluorodopa metabolism measured from the fixed total striatal volume than that from the small ROIs, with the differences being matched by striatal atrophy. However, D_2 losses from aging may be better appreciated in terms of total number of receptors as opposed to receptor density. Therefore, variable striatal ROIs and variable frontal cortex ROIs (to improve potential underestimation of V_2) using MRI coregistration techniques may provide indices that are more accurate for receptor number. However, sensitivity of such measurements in the striatum might be lower because of the partial-volume effect from the limited spatial resolution, compared with those from small ROIs buried well within the striatum. Therefore, in this study, SV ROIs may be considered superior to LV ROIs in modeling age effects.

Age Effect

Our results of age-related losses of D_2 binding are consistent with those of previous PET and postmortem studies (*11–13,29*). In particular, the estimates of D_2 losses per decade, as reported in a PET study by Volkow et al. (*18*), were 7.9% using the striatal distribution volume ratio with ^{11}C-raclopride and 7.8% using the striatal ratio index with ^{18}F-*N*-methylspiroperidol (NMSP). Thus, our estimates using Rv from the SV and the

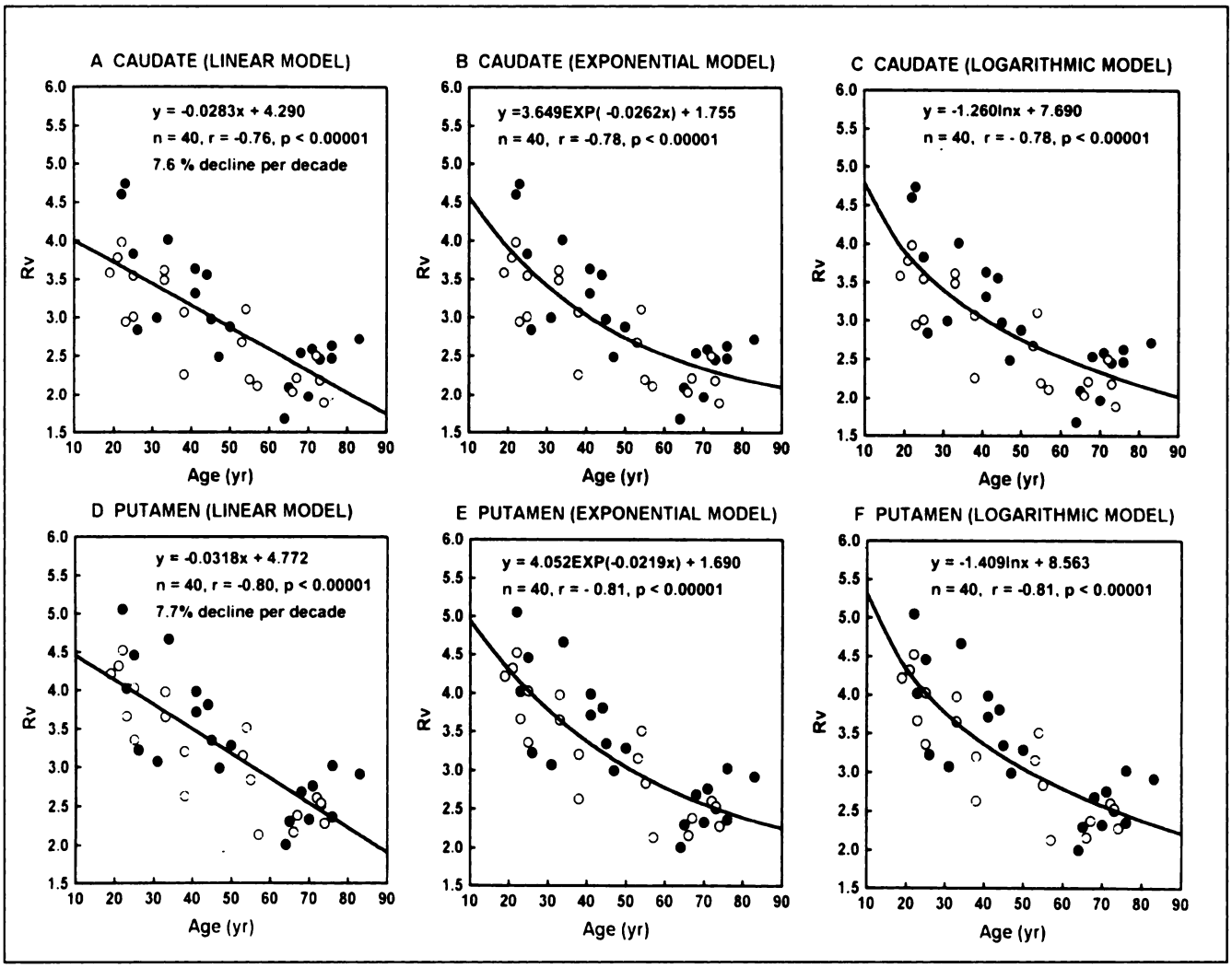

FIGURE 3. (A and D) Line graphs illustrate the relationships between Rv determined from SV ROI set and age by linear model for caudate and putamen, respectively. Solid lines are linear regression. (B, C, E and F) Line graphs illustrate relationships between Rv determined from SV and age by exponential model (B and C) and logarithmic model (E and F) for caudate (B and C) and putamen (E and F), respectively. Solid curves are nonlinear regression. Individual Rv is represented by ● for men and ○ for women, respectively.

linear model (caudate, 7.6%; putamen, 7.7%) closely matched theirs. In addition, our results of slightly higher Rv values for putamen than for caudate and nearly identical age-related changes in the caudate and the putamen generally agree with the results of previous PET and postmortem studies (*11–13,29*), although one postmortem study reported no significant age-related changes in the putamen (*13*). For example, the estimates of D_2 losses per decade (caudate/putamen) were 4%/6% by the PET study and 4.5%/4.8% by the postmortem study, respectively. Thus, aging effects on striatal D_2 binding appear to be regionally nonselective. In Parkinson's disease, on the other hand, dopaminergic neurons projecting to the putamen are more selectively affected by the degenerative process. Consequently, D_2 binding in the putamen but not in the caudate of patients with early Parkinson's disease may be upregulated (*30*).

Using ^{11}C-NMSP, Wong et al. (*14*) showed that age effects on D_2 binding were nonlinear in men but linear in women. In our limited analyses done for men and women separately, we found no major gender differences in age effects on Rv. However, further investigation using larger numbers of subjects

TABLE 3
Quality of Linear and Nonlinear Models to Describe Relationships Between Volume Ratio and Age

	Linear model			Exponential model			Logarithmic model		
Region	$-r^*$	γ	AIC	$-r^*$	γ	AIC	$-r^*$	γ	AIC
Caudate (LV)	0.80	0.64	78.6	0.81	0.65	81.5	0.80	0.64	77.9
Putamen (LV)	0.78	0.60	91.7	0.79	0.62	94.1	0.78	0.61	90.7
Caudate (SV)	0.76	0.58	92.5	0.78	0.61	93.7	0.78	0.60	90.1
Putamen (SV)	0.80	0.64	91.1	0.81	0.66	92.8	0.81	0.66	89.0
Mean	0.78	0.62	88.5	0.80	0.63	90.5	0.79	0.63	87.0
s.d.	0.02	0.03	6.6	0.02	0.03	6.1	0.02	0.03	6.0

*Correlation coefficients expressed in absolute means.
γ = coefficients of determination; AIC = Akaike information criterion; LV = large volume region-of-interest set; SV = small volume region-of-interest set.

may be warranted in view of the evidence in rats of gender differences in estrogen-related effects on D_2 receptor binding (*31*). In other D_2 PET studies and postmortem studies, the linear model mostly was used to characterize age-related changes in D_2 binding. Our slower rates of Rv decline in the elderly (>60 yr) might be partly related to the potential overestimation of Rv because V_2 might be underestimated in the presence of frontal cortical atrophy. However, differential age effects were apparent even at younger ages (<40 yr) (Fig. 3). Separate analyses in our 22 subjects excluding those older than 50 yr showed that the logarithmic model was significantly superior to the other models (data not shown). Although both the logarithmic and exponential models of age effects on D_2 binding appear appropriate in the age range considered in this study, the former may not make biological sense because a logarithmic function would entail very large values at birth and negative values if one lived long enough, whereas the latter may be more plausible because biological systems are known to contain many such examples of an exponential decay. In a recent ^{123}I-(N-3-idopropen-2-yl)-2β-carbomethoxy-3β-(4-chlorophenyl)tropane SPECT study, Mozley et al. (*32*) demonstrated nonlinear effects of age on dopamine transporter binding in the caudate and the putamen. Other imaging studies reported a 6%–8% loss of dopamine transporter binding per decade (*33*). Thus, both the pre- and postsynaptic dopaminergic components may suffer similar effects of age. However, the biological mechanisms underlying the nonlinear effects of age and the apparent relationships between the two components of the dopaminergic system are unclear at this time.

To exclude subjects with potentially undiagnosed extrapyramidal diseases, our subjects older than 50 yr were free of significant extrapyramidal deficits. However, frequent occurrence of subtle extrapyramidal motor dysfunction in the elderly has been suggested to reflect aging of the dopaminergic system. Although reduced D_2 binding is probably contributing to this, we performed no correlation analyses between Rv and motor functions for the following reasons. Extrapyramidal function appears to depend on a complex balance between activities of the cholinergic and dopaminergic systems in the striatum (*34*). For example, Parkinson's disease patients do not develop symptoms of parkinsonism until they have lost 40%–50% of their dopaminergic neurons, presumably because the dopamine deficits are compensated for by the cholinergic activity (*20*). In addition, the tone of the dopaminergic system may be regulated by dopamine transporter-related activity (*35*). Therefore, D_2 binding losses may not correlate directly with extrapyramidal motor deficits, particularly those subtle ones. However, investigations designed to image both the pre- and postsynaptic components of the dopaminergic system concurrently may be warranted to elucidate behavioral consequences of aging effects on this age-vulnerable neurochemical system.

CONCLUSION

IBF SPECT permitted reliable measurement of D_2 binding in the caudate or the putamen separately using small ROI volumes, which significantly improved the quantitation loss from the partial-volume effect. Our results agreed with previous PET and postmortem findings of D_2 binding losses with age. However, our results suggest that the effects of aging may be nonlinear, being progressively smaller with age. Age-related changes in D_2 binding must be taken into consideration in clinical IBF SPECT investigations.

ACKNOWLEDGMENTS

This work was supported in part by the SPECT Research Fund from the Department of Medical Imaging, Mount Sinai Hospital, Toronto, Ontario, Canada; Picker International Canada, Inc., Brampton, Ontario; and a grant from the Medical Research Council of Canada (HT-13367). We thank Douglass Vines for valuable technical assistance. This work was presented in part at the 44th Annual Meeting of the Society of Nuclear Medicine, San Antonio, Texas, June 1–4, 1997.

REFERENCES

1. Ichise M, Ballinger JR. SPECT imaging of dopamine receptors [Editorial]. *J Nucl Med* 1996;37:1591–1595.
2. Brucke T, Podreka I, Angelberger P, et al. Dopamine D_2 receptor imaging with SPECT: studies in different neuropsychiatric disorders. *J Cereb Blood Flow Metab* 1991;11:220–228.
3. Ichise M, Toyama H, Fornazzari L, Ballinger JR, Kirsh JC. Iodine-123-IBZM dopamine D_2 receptor and technetium-99m-HMPAO brain perfusion SPECT in the evaluation of patients with and subjects at risk for Huntington's disease. *J Nucl Med* 1993;34:1274–1281.
4. Buck A, Westera G, Sutter M, Albani C, Kung HF, vonSchulthess GK. Iodine-123-IBF SPECT evaluation of extrapyramidal diseases. *J Nucl Med* 1995;36:1196–1200.
5. Oertel WH, Schwarz J, Tatsch K, Arnold G, Gasser T, Kirsch CM. IBZM-SPECT as predictor for dopamimetic responsiveness of patients with de novo parkinsonian syndrome. *Adv Neurol* 1993;60:519–524.
6. Ichise M, Ballinger JR, Golan H, et al. Noninvasive quantification of dopamine D_2 receptors with iodine-123-IBF SPECT. *J Nucl Med* 1996;37:513–520.
7. Ichise M, Ballinger JR, Vines D, Tsai S, Kung HF. Simplified quantification and reproducibility studies of dopamine D_2-receptor binding with iodine-123-IBF SPECT in healthy subjects. *J Nucl Med* 1997;38:31–37.
8. McGeer PL, McGeer EG, Suzuki JS. Aging and extrapyramidal function. *Arch Neurol* 1977;34:33–35.
9. Kish SJ, Shannak K, Rajput A, Deck JH, Hornykiewicz O. Aging produces a specific pattern of striatal dopamine loss: implications for the etiology of idiopathic Parkinson's disease. *J Neurochem* 1992;58:642–648.
10. De Keyser J, Ebinger G, Vauquelin G. Age-related changes in the human nigrostriatal dopaminergic system. *Ann Neurol* 1990;27:157–161.
11. Seeman P, Bzowej NH, Guan HC, et al. Human brain dopamine receptors in children and aging adults. *Synapse* 1987;1:399–404.
12. Rinne JO. Muscarinic and dopaminergic receptors in the aging human brain. *Brain Res* 1987;404:162–168.
13. Severson JA, Marcusson J, Winbland B, et al. Age-correlated loss of dopaminergic binding sites in human basal ganglia. *J Neurochem* 1982;39:1623–1631.
14. Wong DF, Wagner HN Jr, Dannals RF, et al. Effects of age on dopamine and serotonin receptors measured by positron tomography in the living human brain. *Science* 1984;226:1393–1396.
15. Baron JC, Maziere B, Loc'h C, et al. Loss of striatal [^{76}Br]bromospiperone binding sites demonstrated by positron tomography in progressive supranuclear palsy. *J Cereb Blood Flow Metab* 1986;6:131–136.
16. Rinne JO, Hietala J, Ruotsalainen U, et al. Decrease in human striatal dopamine D_2 receptor density with age: a PET study with [^{11}C]raclopride. *J Cereb Blood Flow Metab* 1993;13:310–314.
17. Antonini A, Leenders KL, Reist H, Thomann R, Beer HF, Locher J. Effect of age on D_2 dopamine receptors in normal human brain measured by positron emission tomography and ^{11}C-raclopride. *Arch Neurol* 1993;50:474–480.
18. Volkow ND, Wang GJ, Fowler JS, et al. Measuring age-related changes in dopamine D_2 receptors with ^{11}C-raclopride and ^{18}F-N-methylspiroperidol. *Psychiatry Res* 1996;67:11–16.
19. Wong DF, Young D, Wilson PD, Meltzer CC, Gjedde A. Quantification of neuroreceptors in the living human brain: III. D_2-like dopamine receptors: theory, validation, and changes during normal aging. *J Cereb Blood Flow Metab* 1997;17:316–330.
20. Fearnley JM, Lees AJ. Aging and Parkinson's disease: substantia nigra regional selectivity. *Brain* 1991;114:2283–2301.
21. Folstein MF, Folstein SE, McHugh PR. "Mini-mental state." A practical method for grading the cognitive state of patients for the clinician. *J Psychiatr Res* 1975;12:189–198.
22. Fahn S, Shoulson I, The Parkinson Study Group. *Unified Rating Scale for Parkinsonism.* Florsham Park, New Jersey: MacMillan; 1987:153–163.
23. Francis PT, Sims NR, Procter AW, Bowen DM. Cortical pyramidal neurone loss may cause glutamatergic hypoactivity and cognitive impairment in Alzheimer's disease: investigative and therapeutic perspectives. *J Neurochem* 1993;60:1589–1604.
24. Talairach J, Tournoux P, Rayport M. *Co-planar stereotaxic atlas of the human brain. 3-dimensional proportional system: an approach to cerebral imaging.* New York: Thieme Inc.; 1988:1–122.
25. Armitage P, Berry G. Comparison of several groups: multiple comparisons. In: *Statistical methods in medical research*, 2nd ed. London: Blackwell Scientific Publications; 1996:200–205.
26. Akaike H. A new look at the statistical model identification. *IEEE Trans Automatic Control* 1974;AC19:716–723.
27. Vingerhoets FJ, Snow BJ, Schulzer M, et al. Reproducibility of fluorine-18-6-fluorodopa positron emission tomography in normal human subjects. *J Nucl Med* 1994;35:18–24.
28. Wang GJ, Volkow ND, Levy AV, et al. MR-PET image coregistration for quantitation of striatal dopamine D_2 receptors. *J Comput Assist Tomogr* 1996;20:423–428.

29. Rinne JO, Lonnberg P, Marjamaki P. Age-dependent decline in human brain dopamine D1 and D_2 receptors. *Brain Res* 1990;508:349–352.
30. Rinne JO, Laihinen A, Ruottinen H, et al. Increased density of dopamine D_2 receptors in the putamen, but not in the caudate nucleus in early Parkinson's disease: a PET study with [^{11}C]raclopride. *J Neurol Sci* 1995;132:156–161.
31. Bazzett TJ, Becker JB. Sex differences in the rapid and acute effects of estrogen on striatal D_2 dopamine receptor binding. *Brain Res* 1994;637:163–172.
32. Mozley PD, Kim HJ, Gur RC, et al. Iodine-123-IPT SPECT imaging of CNS dopamine transporters: nonlinear effects of normal aging on striatal uptake values. *J Nucl Med* 1996;37:1965–1970.
33. Van Dyck CH, Seibyl JP, Malison RT, et al. Age-related decline in striatal dopamine transporter binding with iodine-123-beta-CITSPECT. *J Nucl Med* 1995;36:1175–1181.
34. Ladinsky H, Consolo S, Bianchi S, Ghezzi D, Samanin R. Link between dopaminergic and cholinergic neurons in the striatum as evidenced by pharmacological, biochemical, and lesion studies. In: Garattini S, Pujol JF, Samanin R, eds. *Interactions between putative neurotransmitters in the brain*. New York: Raven Press; 1978:3–21.
35. Donnan GA, Woodhouse DG, Kaczmarczyk SJ, et al. Evidence for plasticity of the dopaminergic system in parkinsonism. *Mol Neurobiol* 1991;5:421–433.

Decreased Benzodiazepine Receptor Binding in Machado-Joseph Disease

Masatoshi Ishibashi, Tetsuo Sakai, Toyojiro Matsuishi, Yoshiharu Yonekura, Yushiro Yamashita, Toshi Abe, Yoshihiro Ohnishi and Naofumi Hayabuchi

Division of Nuclear Medicine and Department of Radiology, Department of Pediatrics and Child Health, Kurume University School of Medicine, Kurume-City; Department of Neurology, National Chikugo Hospital, Fukuoka; Biomedical Imaging Research Center, Fukui Medical School, Fukui; and Nihon Medi-Physics Co., Ltd., Hyogo, Japan

Benzodiazepine receptor binding was assessed in four Japanese men with Machado-Joseph disease. **Methods:** The distribution of benzodiazepine receptors was measured by radionuclide imaging (SPECT) after intravenous administration of ^{123}I-iomazenil (Ro 16-0154). **Results:** SPECT demonstrated decreased binding throughout the cerebral cortex and cerebellum in all patients. Binding potential (receptor concentration × affinity) was diffusely decreased in cerebral cortex, thalamus, striatum and cerebellum compared with control subjects, suggesting that GABAergic function may be decreased globally in these patients. Cerebral blood flow was largely normal, and no cerebral cortical atrophy was evident on MRI. **Conclusion:** Iodine-123-iomazenil SPECT may become a potent method for detecting impairment of the cerebral cortex even before brain perfusion SPECT or MRI can reveal early abnormalities.

Key Words: iodine-123-iomazenil; benzodiazepine receptor; Machado-Joseph disease; SPECT

J Nucl Med 1998; 39:1518–1520

Machado-Joseph disease (MJD) is an autosomal dominant neurodegenerative disorder that was originally described in patients of Portuguese-Azorean ancestry (*1*). Cytidylate, adenylate and guanylate (CAG) expansions in a novel gene at chromosome 14q 32.1 have been discovered in Japanese patients with MJD (*2*). However, the mechanism of central nervous system impairment in such patients is still unknown.

Brain function can be delineated by coupling morphology and receptor imaging (*3*). Imaging of gamma-aminobutyric acid (GABA)/benzodiazepine receptors may help to determine whether GABAergic transmission is impaired in patients with MJD, because the basal ganglia and cerebellum show degeneration in such patients. Iomazenil (Ro 16-0154) is an agonist of benzodiazepine with a high affinity for the central type of benzodiazepine receptor (*4*). This agent can be labeled with ^{123}I without losing binding properties (*5*). Early ^{123}I-iomazenil images primarily reflect blood flow, whereas delayed images taken 3 hr after injection of tracer reflect benzodiazepine receptor binding (*5*).

Received Oct. 28, 1997; revision accepted Dec. 15, 1997.
For correspondence or reprints contact: Masatoshi Ishibashi, MD, Department of Radiology and Division of Nuclear Medicine, Kurume University School of Medicine, 67 Asahi-Machi, Kurume City, Fukuoka, 830-0011, Japan.

MATERIALS AND METHODS

Study Population

Four Japanese men with MJD (age range 34–57 yr, mean 44 yr) were examined (*6*). The diagnosis was confirmed by identification of CAG expansions (*2*). Data from the four patients were compared with those from six healthy age-matched control subjects (age range 24–61 yr, mean 39.7 yr) (*7*). These control subjects gave informed consent.

All four patients with MJD gave informed consent as part of a protocol approved by the Subcommittee on Human Studies at Kurume University School of Medicine. The clinical features of the patients are summarized in Table 1. No benzodiazepine derivatives were administered.

Data Acquisition and SPECT

The labeled receptor ligand ^{123}I-iomazenil was obtained from Nihon Medi-Physics Co. (Nishinomiya, Japan). A bolus of 167 MBq ^{123}I-iomazenil was injected intravenously. SPECT was performed 20 min (early image) and again 3 hr (delayed image) after injection of tracer using a large-field-of-view, dual-detector camera (RC26001; Hitachi, Tokyo, Japan) and a computer system (RW3000; Hitachi) equipped with a low-energy, high-resolution, parallel-hole collimator. The dual-detector camera was rotated over 180° in a circular orbit and in 32 steps of 40 sec each to cover 360° in approximately 22 min. Coronal and sagittal images were derived from the transaxial images. Venous blood samples were drawn 30 min after the radiotracer injection. Ligand-receptor binding was assessed by determining binding potential (Bp), which is defined as a product of the receptor concentration (Bmax) in the brain tissue and the ligand-receptor affinity (1/kD) (*8*). Bp was obtained in the manner reported previously (*9*) for regions of interest corresponding to frontal, occipital, temporal and parietal cortices; thalamus; striatum; and cerebellum. Individual arterial input function was estimated by scaling a standardized shape of time-concentration curve input function and two separate SPECT scans (20 min and 3 hr postinjection) using a table lookup procedure based on a three-compartment, two-parameter kinetic model.

Cerebral blood flow (CBF) images were obtained 20 min after the intravenous injection of 222 MBq ^{123}I-N-isopropyl-p-iodoamphetamine (IMP) using the same equipment and data processing as those for ^{123}I-iomazenil images.